

# Synthesis and microstructural characterization of $\text{Bi}_{12}\text{SiO}_{20}$ (BSO) thin films produced by the sol–gel process

Asja Veber\*, Špela Kunej, Danilo Suvorov

*Institut Jožef Stefan, Jamova 39, 1000 Ljubljana, Slovenia*

Received 6 April 2009; received in revised form 24 June 2009; accepted 25 July 2009

Available online 25 August 2009

## Abstract

We have produced  $\text{Bi}_{12}\text{SiO}_{20}$  (BSO) thin films using the sol–gel process. The stable sol was synthesized using  $\text{Bi}(\text{NO}_3)_3 \cdot 5\text{H}_2\text{O}$  and  $\text{Si}(\text{OC}_2\text{H}_5)_4$  (TEOS) as the precursors, acetic acid and 2-ethoxyethanol as the solvents, and ethanolamine as the stabilizer. The stability of the solution, which depends on the concentration and the  $R_h$  value ( $R_h = [\text{H}_2\text{O}]/[\text{M}]$ ), directly affects the microstructure of the BSO thin film. We determined that the optimal concentration for the preparation of BSO thin films is 0.76 M. The influences of the substrates, the annealing temperature, the concentration and the  $R_h$  = value of the solution on the microstructure of the  $\text{Bi}_{12}\text{SiO}_{20}$  thin films were investigated. X-ray diffraction (XRD) showed that the  $\text{Bi}_{12}\text{SiO}_{20}$  starts to form at 500 °C and that single-phase  $\text{Bi}_{12}\text{SiO}_{20}$  polycrystalline thin films are formed at 700 °C. The coated films were characterized by means of X-ray diffraction (XRD), scanning electron microscopy (SEM) and atomic force microscopy (AFM).

© 2009 Elsevier Ltd and Techna Group S.r.l. All rights reserved.

**Keywords:** A. Sol–gel process; Thin film;  $\text{Bi}_{12}\text{SiO}_{20}$

## 1. Introduction

Low-temperature co-fired ceramics (LTCC) technology has become crucial in the development of various modules and substrates in wireless microwave applications. This technology has advantages in comparison with other technologies, for example, the ceramics are fired below 900 °C, which permits co-firing with highly conductive and less-expensive electrode metals. LTCC technology also permits the embedding of passive elements, such as resistors, capacitors and inductors, into a ceramics package, and so the size of the resulting module can be made smaller.

Bismuth silicon oxide,  $\text{Bi}_{12}\text{SiO}_{20}$  (BSO), belongs to the sillenite family, with the general formula  $\text{Bi}_{12}\text{MO}_{20}$  ( $\text{M} = \text{Si}, \text{Ge}, \text{Ti}, \text{Pb}, \text{Mn}, \text{B}_{1/2}\text{P}_{1/2}$ ), which is considered to be a promising material in LTCC technology, because of its piezoelectric, electro-optic, photo-refractive and optically active properties [1]. BSO is a stoichiometric sillenite with a fully occupied oxygen sublattice that meets all the major criteria for application in LTCC modules, such as a low sintering

temperature ( $T_s = 850$  °C) as well as a chemical compatibility with metal electrodes and other functional ceramics [2]. The dielectric properties of BSO include low dielectric losses and a sufficiently suppressed temperature coefficient of resonant frequency  $\tau_f$  [2]. Because of the current trend towards miniaturization, which demands a reduction in the thickness of the dielectric layer, a lot of attention has been focused over the past 10 years on the preparation of dielectric thin films using the sol–gel method [3–10]. Sol–gel synthesis appears to be very promising, since it offers potential advantages over traditional solid-state synthesis methods. In particular, the lower processing temperatures [7–11] might facilitate its use in LTCC technology. In addition, the sol–gel method allows a precise control over the composition, the homogeneity and deposition over a large area. However, the most important advantage of sol–gel synthesis in comparison with other coating methods is the ability to tailor the microstructure of the deposited film by varying the concentration, the pH, the  $R_h$  value and the viscosity of the sol [11–13]. The grain size and the porosity of the thin films have a significant influence on their functional properties, which means it is very important to optimize the synthesis parameters for the deposition of these thin films. Generally, three reactions are used to describe the sol–gel method: hydrolysis, alcohol condensation, and water condensation. In

\* Corresponding author. Tel.: +386 1 477 39 92; fax: +386 1 477 38 75.

E-mail address: [asja.veber@ijs.si](mailto:asja.veber@ijs.si) (A. Veber).

the hydrolysis reaction the alkoxide group (OR) is replaced by a hydroxyl group (OH). Subsequently, condensation reactions involving silanol (Si–OH) groups produce siloxane bonds (Si–O–Si) and the by-product is alcohol or water. Condensation begins as soon as the ((OR)<sub>3</sub>Si–OH) groups are formed; therefore, the hydrolysis and condensation are often concurrent reactions. The condensation reaction leads to the growth of the structure by the formation of Si–O–Si bonds, and then when the condensation is complete, the gel forms [14].

BSO thin films have already been successfully synthesized by chemical vapor deposition (CVD) [15,16], the sol–gel process [17,18] and pulsed-laser deposition (PLD) [19,20]. However, there is no information in the literature [17,18] about the influence of the synthesis parameters, such as the  $R_h$  value, the ageing time of the sols, and the substrate, on the microstructural development of BSO thin films formed by the sol–gel process. The hydrolysis rate  $R_h = [H_2O]/[M]$ , where M is the metal cation in the alkoxide, describes the relative amount of water present in the sol. The extent of the hydrolysis and the condensation, and hence the structure of the alkoxide-based precursor in the coating solution, depends on  $R_h$ , together with the ageing time, the concentration and the catalyst or additive content. Higher  $R_h$  values ordinarily lead to gelation in a shorter time and therefore a less dense microstructure for the thin films [12]. The ageing time is also a parameter that determines the microstructure. The post-deposition variation in the properties of thin films as a function of time is referred to as the ageing time  $t_G$ .

Our research was focused on the synthesis of BSO thin films, using the sol–gel method, deposited on various substrates – MgAl<sub>2</sub>O<sub>4</sub> (spinel), sapphire and Si/SiO<sub>2</sub>/TiO<sub>2</sub>/Pt – using the spin-coating method. The substrates were chosen on the basis of their cell parameters and possible future applications. In this paper the influence of the precursor solution, the  $R_h$  value, the concentration of the solution and the type of substrate on the microstructural development of Bi<sub>12</sub>SiO<sub>20</sub> thin films is discussed.

## 2. Experimental

The sol was prepared using bismuth nitrate Bi(NO<sub>3</sub>)<sub>3</sub>·5H<sub>2</sub>O (Alfa Aesar, 98%) and tetraethyl orthosilicate Si(OC<sub>2</sub>H<sub>5</sub>)<sub>4</sub> (Alfa Aesar, 98%) as the precursors, 2-ethoxyethanol (Alfa Aesar, 99%) and glacial acetic acid (Alfa Aesar, 99.7+%) as the solvents and ethanolamine (Alfa Aesar, 98%) as the complex agent. The 98% pure Bi(NO<sub>3</sub>)<sub>3</sub>·5H<sub>2</sub>O (10 g) was dissolved in the acetic acid (20.4 ml) and the ethanolamine (4 ml) was added to protect the bismuth ions from hydrolysis. This was followed by the addition of tetraethyl orthosilicate (0.38 ml) under constant stirring for 5 h at room temperature. The precursor solution was then diluted with 2-ethoxyethanol to the concentration range from 0.48 to 1.20 M. The sols were prepared with  $R_h = H_2O/TEOS$  molar ratios of 5 and 60 (referred to as  $R_h$  5 and  $R_h$  60). Due to the large amount of water in Bi(NO<sub>3</sub>)<sub>3</sub>·5H<sub>2</sub>O ( $R_h$  60) we decided to decrease the  $R_h$  by drying the Bi(NO<sub>3</sub>)<sub>3</sub>·5H<sub>2</sub>O. Consequently, the Bi(NO<sub>3</sub>)<sub>3</sub>·5H<sub>2</sub>O was vacuum dried to obtain sols with  $R_h$  5. The sols were then

filtered through 0.2-μm filters and deposited onto various substrates, such as Pt/TiO<sub>2</sub>/SiO<sub>2</sub>/Si, sapphire and MgAl<sub>2</sub>O<sub>4</sub> (spinel), using the spin-coating method with 5000 rpm for 30 s.

Each layer was heated on a hot plate for 2 min at 220 °C to pyrolyze the residual solvents before the deposition of the next layer. The so-produced thin films consisting of different numbers of layers were annealed at 700 °C for 1 h.

X-ray diffraction (XRD, ENDEAVOR, D4, Bruker, AXS) was used to analyze the phase formation of the thin films. The microstructures of the films were investigated with scanning electron microscopy (SEM, JEOL 8500A, Japan) and atomic force microscopy (AFM, VEECO DIMENSION 3100). The grain size of the thin films was estimated from SEM-SEI (secondary electron) micrographs.

## 3. Results and discussion

Good control over the synthesis parameters is needed to obtain a dense BSO thin film. The microstructure development of a BSO thin film depends significantly on the synthesis conditions, such as the concentration of the solution, which has an impact on its ageing behavior, the  $R_h$  value, the annealing temperature and the texture of the substrate [6,8].

### 3.1. Influence of sol concentration and ageing of the solution on the microstructure of the BSO thin film

To optimize the concentrations of the  $R_h$  60 and  $R_h$  5 sols for the deposition of the BSO thin films, sols with concentrations ranging from 0.48 to 1.20 M were synthesized. Fig. 1 shows the influence of the concentration of the  $R_h$  5 and  $R_h$  60 sols on the ageing time of the sols. The results indicated that the  $R_h$  60 sol with a concentration of 1.2 M is stable for 5 h before the gel forms, while the  $R_h$  60 sol with a concentration of 0.76 M is stable for a much longer period, i.e., 450 h. In contrast, the  $R_h$  60 sols with a concentration 0.67 M and below were unstable due to the re-crystallization of the bismuth nitrate. The  $R_h$  5 sols were stable across the whole concentration range due to protection of bismuth ions with ethanolamine, forming a

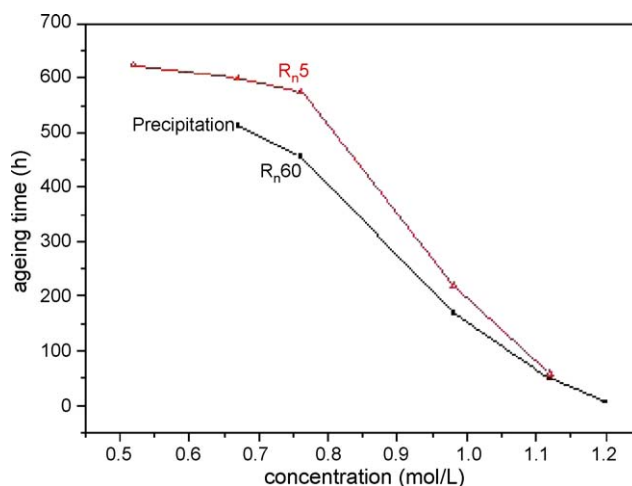


Fig. 1. Stability graph for the  $R_h$  60 and  $R_h$  5 sols.

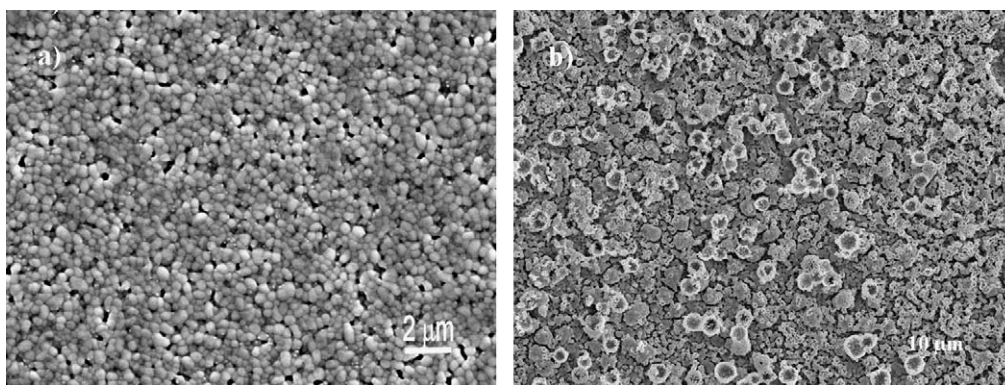


Fig. 2. SEM images of microstructures of BSO thin films deposited from sol ( $R_h$  5;  $c = 0.76$  M, 5000 rpm) on sapphire substrates annealed at  $700^\circ\text{C}$  for 1 h: (a) a fresh solution and (b) an aged solution (24 days).

bismuth complex, which prevents the hydrolysis of the trivalent bismuth ion [21]. The ageing time for the  $R_h$  5 sol with a concentration of 1.20 M was 220 h, while the  $R_h$  5 sols with a concentration of 0.48 M become a gel in 723 h.

We chose the  $R_h$  60 and  $R_h$  5 sols with the same concentration, 0.76 M, for the investigation of the influence of the synthesis parameters on BSO thin films. Both sols,  $R_h$  60 and  $R_h$  5, with this concentration have the longest gelation times,  $t_G = 450$  h and  $t_G = 700$  h, respectively. The  $R_h$  5 sols with a concentration below 0.76 M do have a longer gelation time, but not significantly longer, and therefore the effect on the microstructural development is minimal.

We observed that the ageing time of the solution is a variable that has a significant effect on the final microstructure development of BSO thin films. The repeatability of the deposition procedure depends on the sol's ageing-rate. The microstructures of the thin films deposited on sapphire substrates from (a) a fresh solution and (b) a solution aged for 14 days are shown in Fig. 2. The films were annealed at  $700^\circ\text{C}/1$  h, because with this annealing condition the sillenite phase was obtained, see Section 3.3.

The microstructure of the BSO thin film deposited from a fresh solution (Fig. 2a) shows a well-defined grain shape with the grains being 300 nm in size. Fig. 2(b) shows a non-uniform microstructure development due to the increased ageing time of

the solution, which means that a uniform, dense thin film cannot be obtained. From this result we concluded that for a homogeneous BSO thin film we must prepare it from a solution before the ageing starts. With respect to the ageing we investigated several substrates, i.e., Pt/TiO<sub>2</sub>/SiO<sub>2</sub>/Si, sapphire and MgAl<sub>2</sub>O<sub>4</sub>, and for all of them the results were comparable.

### 3.2. Influence of $R_h$ value on the microstructure of a BSO thin film

The  $R_h$  value ( $R_h = \text{H}_2\text{O}/\text{TEOS}$ ) is another parameter that affects the microstructural development of BSO thin films. Thin films from sols with  $R_h$  60,  $c = 0.76$  M and  $R_h$  5,  $c = 0.76$  M were prepared and are shown in Fig. 3. The microstructure of the thin film deposited on Pt/TiO<sub>2</sub>/SiO<sub>2</sub>/Si from the  $R_h$  60 sol (Fig. 3a) shows a high porosity; meanwhile, the BSO thin film deposited from the  $R_h$  5 sol shows a much higher density and a more uniform microstructure that consists of grains with an average size of 500 nm (Fig. 3b). It is known that the evaporation and the attendant capillary force compact the structure, while the condensation reaction stiffened the gel network and caused a high resistance to flow [3]. As mentioned previously (see Section 3.1), the higher  $R_h$  value leads to gelation of the thin film in a shorter time (Fig. 1). Therefore, when depositing the  $R_h$  60 sol on the substrates, the gelation of

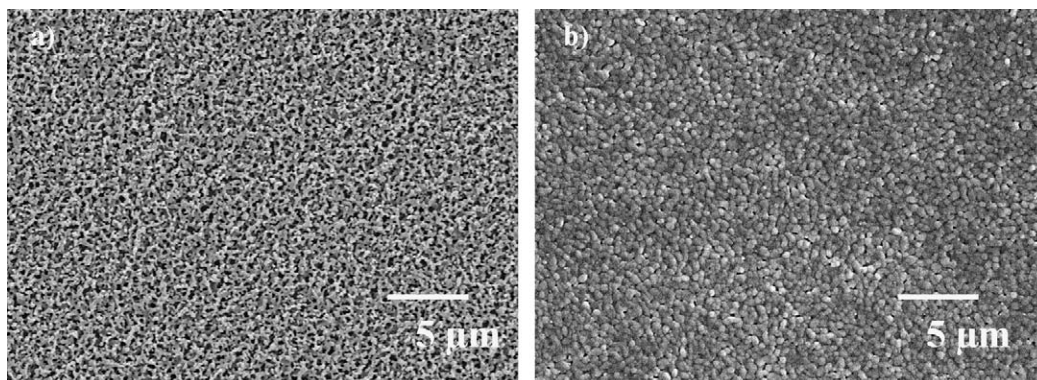


Fig. 3. SEM images of BSO thin films annealed at  $700^\circ\text{C}$ , 1 h deposited on a Pt/TiO<sub>2</sub>/SiO<sub>2</sub>/Si substrate from solutions with (a)  $R_h$  60 ( $c = 0.76$  M, 5000 rpm) and (b)  $R_h$  5 ( $c = 0.76$  M, 5000 rpm).



the deposited thin film occurs much more quickly than the evaporation of the solvent and the film becomes a gel before it dries. This causes a large amount of solvent to be trapped in the thin film, which results in the formation of a lot of porosity in the microstructure after the heat treatment, as shown in Fig. 3a. We believe that the competition between the evaporation of the solvent and the condensation defines the microstructure of the coating. Similar results were obtained for the BSO thin films deposited on the spinel and sapphire substrates.

### 3.3. Influence of annealing temperature on the phase evolution

We found that the annealing temperature has a significant influence on the phase evolution of the thin film. In order to follow the phase formation of the BSO phase we analyzed the X-ray diffraction pattern of a thin film deposited on a sapphire substrate and annealed at temperatures ranging from 300 to 700 °C. The results of the X-ray analysis are shown in Fig. 4. After the deposition of the sol with a concentration of 0.76 M on a substrate the solvent started to evaporate and the gel formed. During the drying and heating of the thin films the organic part decomposes and the amorphous layer transforms into a crystalline oxide coating. At 300 °C we observed the presence of silicon oxide (melanophlogite) and bismuth oxide phases. An increased annealing temperature of up to 400 °C

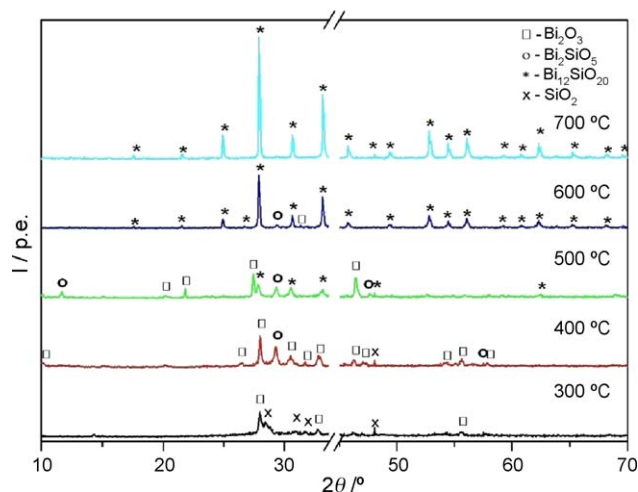


Fig. 4. X-ray diffraction patterns of BSO thin films deposited on a sapphire substrate and heated at various temperatures.

leads to a decreased intensity of the silicon oxide peaks, while new reflections appear, indicating the formation of the bismuth silicate phase ( $\text{Bi}_2\text{SiO}_5$ ), which confirms a reaction between the bismuth oxide and the silicon oxide. After heating at 500 °C, the formation of a new phase, BSO, was confirmed. With the appearance of the BSO phase the amount of bismuth silicate phase and bismuth oxide phase decreased, indicating that the

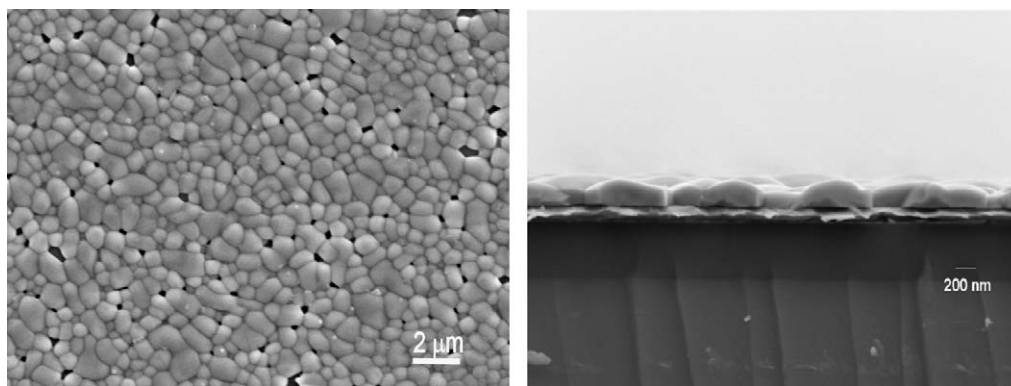


Fig. 5. SEM images of the microstructures and cross-sections of BSO thin films prepared at 700 °C for 1 h, deposited from the  $R_h$  5 sol ( $c = 0.75$  M, 5000 rpm) on a Pt/TiO<sub>2</sub>/SiO<sub>2</sub>/Si substrate.

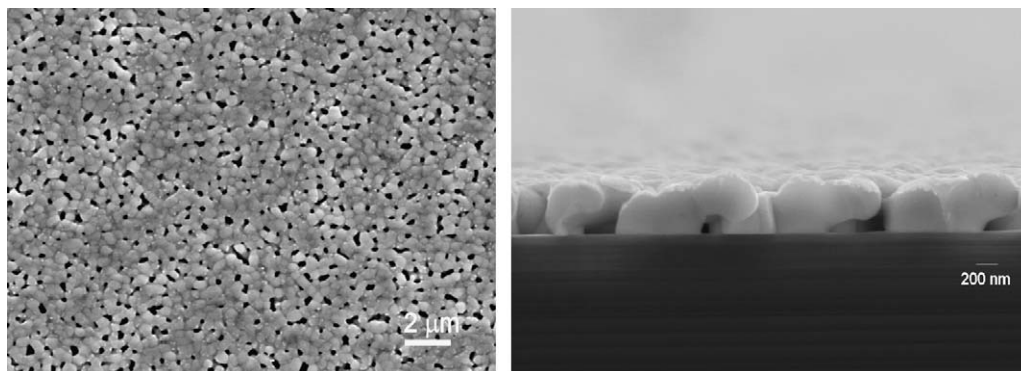


Fig. 6. SEM images of the microstructures and cross-sections of BSO thin films prepared at 700 °C for 1 h, deposited from the  $R_h$  5 sol ( $c = 0.75$  M, 5000 rpm) on a sapphire substrate.

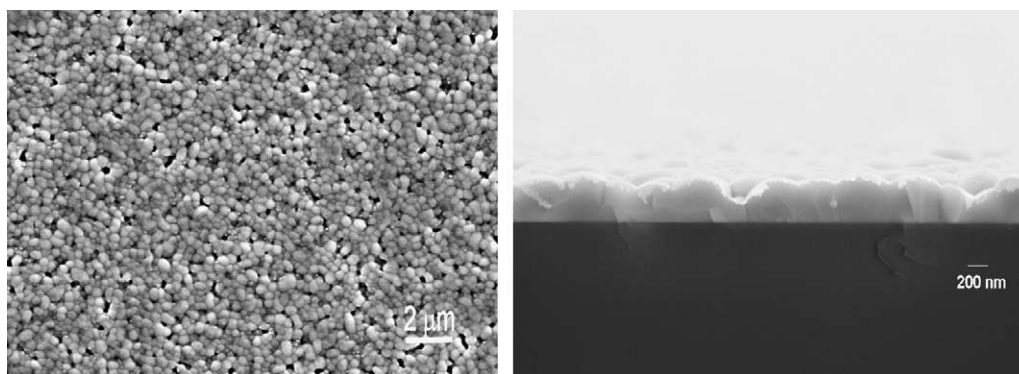


Fig. 7. SEM images of the microstructures and cross-sections of BSO thin films prepared at 700 °C for 1 h, deposited from the  $R_h$  5 sol ( $c = 0.75$  M, 5000 rpm) on a spinel substrate.

BSO forms from a reaction between the bismuth silicate phase and the bismuth oxide phase. At 600 °C the majority of the reflections belong to the sillenite phase; however, there are still traces of the bismuth oxide and bismuth silicate phases present. When the annealing temperature was increased to 700 °C the only detected phase was BSO. From this we can conclude that the annealing temperature to obtain pure BSO thin films is 700 °C. Under these annealing conditions no evaporation or sublimation of  $\text{Bi}_2\text{O}_3$  from the thin films was observed, as only the pure BSO phase formed and no secondary Bi-deficient phases were detected. The same phase evolution was observed for the spinel and  $\text{Pt/TiO}_2/\text{SiO}_2/\text{Si}$  substrates.

#### 3.4. Influence of the substrate on the microstructure of a $\text{Bi}_{12}\text{SiO}_{20}$ thin film

It is known that several parameters can influence the growth of thin films on a substrate, among them the most important are the lattice match or the mismatch between the film and the substrate [10], defects on the surface of the substrate (dislocations, hillocks, etc.), surface and interfacial energies, the elastic strain energy of the thin film and the substrate, dust on the substrate and other contaminants in the solution, etc. [6]. The surface energy in very thin films produced from dilute solutions is believed to be the driving force that determines the texture [22]. In contrast, a

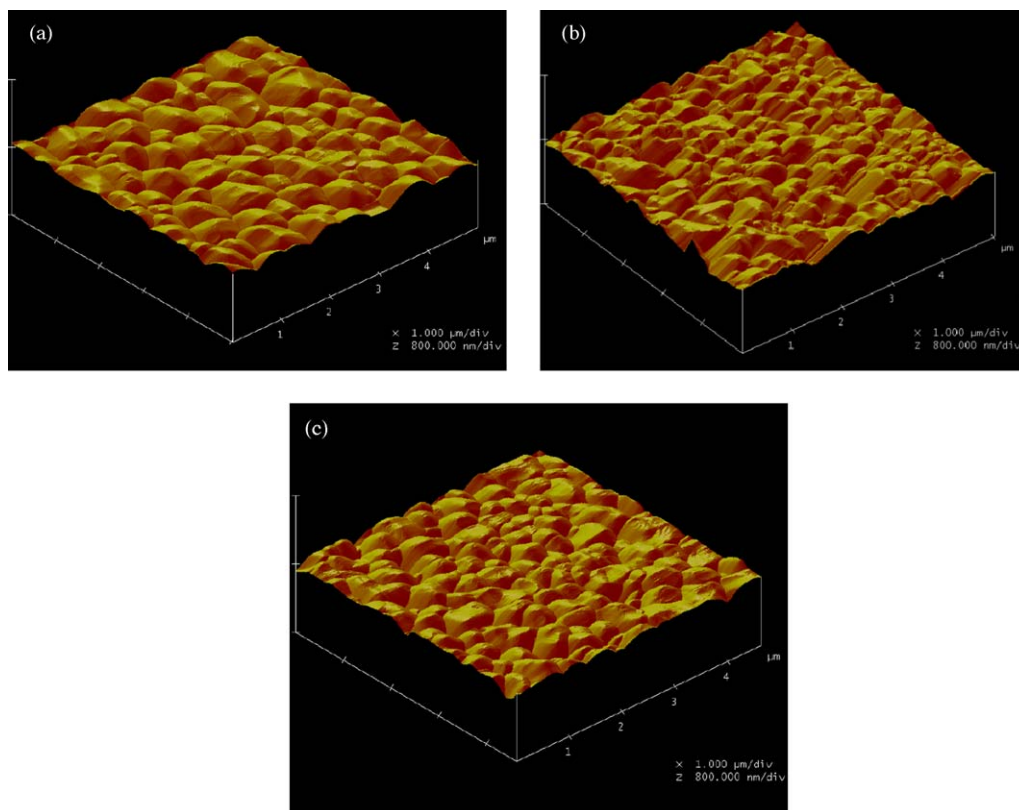


Fig. 8. AFM micrographs of BSO thin films annealed at 700 °C, deposited from the  $R_h$  5 sol ( $c = 0.75$  M, 5000 rpm) on (a)  $\text{Pt/TiO}_2/\text{SiO}_2/\text{Si}$ , (b) sapphire and (c) spinel substrates.

more concentrated and viscous solution or the deposition of more than one layer produces thicker films, which are less affected by the surface energies. Therefore, multiple depositions of cubic BSO ( $a = 10.11 \text{ \AA}$ ) thin films were made from concentrated sol solutions ( $c = 0.76 \text{ M}$ ), at 5000 rpm, on substrates which have cubic ( $\text{Pt/TiO}_2/\text{SiO}_2/\text{Si}$ ,  $a = 3.97 \text{ \AA}$  and spinel,  $a = 8.08 \text{ \AA}$ ) and hexagonal (sapphire,  $a = 4.75 \text{ \AA}$ ,  $c = 12.98 \text{ \AA}$ ) crystal structures. Figs. 5–7 show SEM photographs of the microstructures and cross-sections of  $\text{Bi}_{12}\text{SiO}_{20}$  thin films prepared on  $\text{Pt/TiO}_2/\text{SiO}_2/\text{Si}$ , sapphire and spinel substrates and annealed at  $700^\circ\text{C}$ , 1 h. On the  $\text{Pt/TiO}_2/\text{SiO}_2/\text{Si}$  substrate we obtained a thickness of 200 nm, on the sapphire substrate, 400 nm, while on the spinel substrate the thickness of the BSO thin film was 300 nm.

Fig. 5 shows the homogeneous microstructure of the BSO thin film on a  $\text{Pt/TiO}_2/\text{SiO}_2/\text{Si}$  substrate; deposited from a fresh solution, by spin-coating at 5000 rpm and then annealing at  $700^\circ\text{C}$ , for 1 h. Grains with an average size of 500 nm are observed and the presence of pores is apparent. The microstructures of the BSO thin films deposited on sapphire substrates, as shown in Fig. 6, implied that using this particular precursor sol and these deposition conditions does not result in obtaining a dense BSO thin film on the sapphire substrate. Meanwhile, the microstructure of a BSO thin film deposited on a spinel substrate, as shown in Fig. 7, shows grains with an average size of 200 nm and a reasonably dense microstructure.

The surface roughness of the BSO thin films was determined using atomic force microscopy. Fig. 8 shows an atomic force micrograph of BSO thin films annealed at  $700^\circ\text{C}$  for 1 h deposited on  $\text{Pt/TiO}_2/\text{SiO}_2/\text{Si}$ , sapphire and spinel substrates. On the  $\text{Pt/TiO}_2/\text{SiO}_2/\text{Si}$  and spinel substrates the surfaces of the BSO thin films appear to be smooth, while on the sapphire substrate the surface is relatively rough. The roughness measured by AFM ranged from 50 to 60 nm for the  $\text{Pt/TiO}_2/\text{SiO}_2/\text{Si}$  substrate and 20–30 nm for the spinel substrate, while the roughness of the BSO thin film deposited on the sapphire substrate was as high as 100–120 nm.

#### 4. Conclusions

$\text{Bi}_{12}\text{SiO}_{20}$  thin films were synthesized on various substrates, using the sol–gel method, and annealed at  $700^\circ\text{C}$ . We found that the morphology of the film was affected by the  $t_G$  and the  $R_h$  values of the precursor solution. Thin films with a low porosity resulted from a fresh sol with  $R_h$  5. The investigation of the influence of different substrates on the microstructural development revealed that  $\text{Pt/TiO}_2/\text{SiO}_2/\text{Si}$  as a substrate led to the formation of a homogeneous and dense BSO thin film of thickness  $\cong 200 \text{ nm}$ . The thin film deposited on the spinel substrate also showed a homogeneous microstructure with a thickness of 300 nm, while the BSO thin film deposited on the sapphire substrate resulted in a porous thin-film formation with a rough surface and a thickness of 400 nm.

#### References

- [1] R.E. Aldrich, S.L. Hou, M.L. Harvill, Electrical and optical properties of  $\text{Bi}_{12}\text{SiO}_{20}$ , *J. Appl. Phys.* 42 (1971) 493–494.
- [2] M. Valant, D. Suvorov, Processing and dielectric properties of sillenite compounds  $\text{Bi}_{12}\text{MO}_{20-\delta}$  ( $M = \text{Si, Ge, Ti, Pb, Mn, Bi}_{1/2}\text{P}_{1/2}$ ), *J. Am. Ceram. Soc.* 84 (2001) 2900–2904.
- [3] S. Madeswaran, N.V. Giridharan, R. Jayavel, Sol–gel synthesis and property studies of layered perovskite bismuth titanate thin films, *Mater. Chem. Phys.* 80 (2003) 23–28.
- [4] S. Song, J. Zhai, X. Yao, Effects of buffer layer on the dielectric properties of  $\text{BaTiO}_3$  thin films prepared by sol–gel processing, *Mater. Sci. Eng. B* 145 (2007) 28–33.
- [5] L.B. Kong, J. Ma, Randomly oriented  $\text{Bi}_4\text{Ti}_3\text{O}_{12}$  thin films derived from a hybrid sol–gel process, *Thin Solid Films* 379 (2000) 89–93.
- [6] P. Fuierer, B. Li, Nonepitaxial orientation in sol–gel bismuth titanate films, *J. Am. Ceram. Soc.* 85 (2002) 299–304.
- [7] S.U. Adikory, H.L.W. Chan, Ferroelectric and dielectric properties of sol–gel derived  $\text{Ba}_x\text{Sr}_{1-x}\text{TiO}_3$  thin films, *Thin Solid Films* 424 (2003) 70–74.
- [8] A.V. Prasadarao, U. Selvaraj, S. Komarneni, A.S. Bhala, Fabrication of  $\text{La}_2\text{Ti}_2\text{O}_7$  thin films by sol–gel technique, *Ferroelectr. Lett.* 14 (1992) 65–72.
- [9] U. Selvaraj, A.V. Prasadarao, S. Komarneni, Sol–gel processing of oriented  $\text{PbTiO}_3$  thin films with lead acetylacetonate as the lead precursor, *Mater. Lett.* 20 (1994) 71–74.
- [10] D.S. Paik, A.V. Prasadarao, S. Komarneni, Sol–gel fabrication of PZT thin films: effect of buffer layer in promoting epitaxial growth, *Ferroelectrics* 211 (1998) 141–151.
- [11] B. Malič, Solution processing of electroceramics, in: *Processing of Electroceramics Symposium*, 2003, 41–42.
- [12] N.B. Dahotre, T.S. Sudarshan, *Intermetallic and Ceramic Coatings*, Marcel Dekker, Inc., Switzerland, 1999.
- [13] J.K. Hong, H.R. Kim, H.H. Park, The effect of sol viscosity on the sol–gel derived low density  $\text{SiO}_2$  xerogel film for intermetal dielectric application, *Thin Solid Films* 332 (1998) 449–454.
- [14] C.J. Brinker, G.W. Scherer, *Sol–Gel Science: The Physics and Chemistry of Sol–Gel Processing*, Academic Press, San Diego, CA, 1989.
- [15] Y.N. Nagao, Y. Mimura, Epitaxial growth of  $\text{Bi}_{12}\text{SiO}_{20}$  films by chemical vapor deposition, *Jpn. J. Appl. Phys.* 24 (1985) 954–955.
- [16] M. Jain, A.K. Tripathi, T.C. Goel, P.K.C. Pillai, Preparation and characterization of bismuth silicate (BSO) thin film by the sol–gel technique, *J. Mater. Sci. Lett.* 18 (1999) 479–481.
- [17] E.O. Klebanski, A.Yu. Kudzin, V.M. Pasal' ski, S.N. Plyaka, L.Ya. Sadovskaya, G.Kh. Sokolyanski, Thin sol–gel bismuth silicate films, *Phys. Solid State* 41 (1999) 913–915.
- [18] S.N. Plyaka, G.Ch. Sokolyanskii, E.O. Klebanski, Conductivity of  $\text{Bi}_{12}\text{SiO}_{20}$  thin films, *Condens. Matter Phys.* 2 (1999) 625–630.
- [19] T. Okada, F. Yahiro, H. Uetohara, Y. Nakata, M. Maeda, S. Higuchi, Deposition of highly oriented  $\text{Bi}_{12}\text{SiO}_{20}$  thin films on Y-stabilized zirconia and  $\text{SiO}_2$  by pulsed-laser deposition, *Appl. Phys. A* 69 (1999) 723–726.
- [20] J.C. Alonso, R. Diamant, E. Haro-Poniatowski, M. Fernandez-Guasti, G. Munoz, I. Camarillo, M. Jouanne, J.F. Morhange, Raman characterization of  $\text{Bi}_{12}\text{SiO}_{20}$  thin films obtained by pulsed laser deposition, *Appl. Surf. Sci.* 109–110 (1997) 359–361.
- [21] H. Gu, W. Cao, R. Song, X. Zhou, J. Wang, Effects of precursor solution pH value and substrate texture on orientation degree of sol–gel derived bismuth titanate thin films, *Phys. State Sol.* 198 (2003) 282–288.
- [22] M.M. Sandstrom, P. Fuierer, Influence of nanoparticle seeding on the phase formation kinetics of sol–gel-derived  $\text{Sr}_{0.7}\text{Bi}_{2.4}\text{Ta}_2\text{O}_9$  thin films, *J. Mater. Res.* 18 (2003) 387–395.